

# BIOCHEMICAL JOURNAL

## ACCEPTED MANUSCRIPT

Interrogation of a Lacrimo-auriculo-dento-digital syndrome protein reveals novel modes of Fibroblast growth factor 10 (FGF10) function

Marta Mikolajczak, Timothy Goodman and Mohammad K. Hajihosseini

Heterozygous mutations in the gene encoding fibroblast growth factor 10 (FGF10) or its cognate receptor, FGF-receptor 2 IIIb (FGFR2-IIIb) result in two human syndromes - LADD (lacrimo-auriculo-dento-digital) and ALSG (Aplasia of lacrimal and salivary glands). To date, the partial loss-of-FGF10 function in these patients has been attributed solely to perturbed paracrine signalling functions between FGF10-producing mesenchymal cells and FGF10-responsive epithelial cells. However, the functioning of a LADD-causing G138E FGF10 mutation, which falls outside its receptor interaction interface, has remained enigmatic. In this study, we interrogated this mutation in the context of FGF10's protein sequence and threedimensional structure, and followed the subcellular fate of tagged proteins containing this or other combinatorial FGF10 mutations, *in vitro*. We report that FGF10 harbours two putative nuclear localization sequences, termed NLS1 and NLS2, which individually or co-operatively promote nuclear translocation of FGF10. Furthermore, FGF10 localizes to a subset of dense fibrillar components of the nucleolus. G138E falls within NLS1 and abrogates FGF10's nuclear translocation whilst attenuating its progression along the secretory pathway. Our findings suggest that in addition to its paracrine roles, FGF10 may normally play intracrine role/s within FGF10-producing cells. Thus, G138E may disrupt both paracrine and intracrine function/s of FGF10 through attenuated secretion and nuclear translocation, respectively.

Cite as *Biochemical Journal* (2016) DOI: 10.1042/BCJ20160441

**Copyright 2016 The Author(s).**

Use of open access articles is permitted based on the terms of the specific Creative Commons Licence under which the article is published. Archiving of non-open access articles is permitted in accordance with the Archiving Policy of Portland Press (<http://www.portlandpresspublishing.com/content/open-access-policy#Archiving>).

# **Interrogation of a Lacrimo-auriculo-dento-digital syndrome protein reveals novel modes of Fibroblast growth factor 10 (FGF10) function**

Marta Mikolajczak\*, Timothy Goodman\* and Mohammad K. Hajihosseini<sup>‡</sup>

School of Biological Sciences, University of East Anglia, Norwich, NR4 7TJ, UK

\* Equal contribution

<sup>‡</sup> Corresponding author: [m.k.h@uea.ac.uk](mailto:m.k.h@uea.ac.uk)

Address for correspondence:

Mohammad K. Hajihosseini PhD

School of Biological Sciences,

University of East Anglia,

Norwich, NR4 7TJ, United Kingdom

Tel: +44 (1603) 591318

Fax: +44 (1603) 592250

Short Title: LADD protein analysis reveals novel modes of FGF10 function

Key words: LADD, mutation, nuclear localization, FGF10, paracrine, autocrine.

Abbreviations (in alphabetical order):

ALSG – aplasia of lacrimal and salivary glands syndrome

ARPE – human retinal pigment epithelial cells

ATDC5 – chondrogenic mesenchymal cells

$\beta$ COP – coat protein (coatomer)  $\beta$

$\beta$ -Kap –  $\beta$ -karyopherin, also called importin-  $\beta$

DFC – dense fibrillar components

ER – endoplasmic reticulum  
ERp60 – an isoform of Protein disulphide-isomerase  
FGF – fibroblast growth factor  
FGFR – fibroblast growth factor receptor  
GAPDH – glyceraldehyde 3-phosphate dehydrogenase  
H-bond – hydrogen bonds  
HA – Hemagglutinin A  
HMW – high molecular weight  
LADD – lacrimo-auriculo-dento-digital syndrome  
LMW – low molecular weight  
M phase – mitosis phase of cell cycle  
NLS – nuclear localisation sequence  
NoBP – nucleolar binding protein  
PNGase F – Peptide -N-Glycosidase F  
RT-PCR – reverse transcription polymerase chain reaction  
SDS – sodium dodecyl sulfate  
SMAD – amalgam of ‘mothers against decapentaplegic’ (MAD) (*Drosophila*) and ‘small body size’ (SMA) (*C.elegants*)  
TGN46 – trans-Golgi network integral membrane protein 2  
UBF – upstream binding factor  
WT – wild type

## **ABSTRACT**

Heterozygous mutations in the gene encoding fibroblast growth factor 10 (FGF10) or its cognate receptor, FGF-receptor 2 IIIb (FGFR2-IIIb) result in two human syndromes - LADD (lacrimo-auriculo-dento-digital) and ALSG (Aplasia of lacrimal and salivary glands). To date, the partial loss-of-FGF10 function in these patients has been attributed solely to perturbed paracrine signalling functions between FGF10-producing mesenchymal cells and FGF10-responsive epithelial cells. However, the functioning of a LADD-causing G138E FGF10 mutation, which falls outside its receptor interaction interface, has remained enigmatic. In this study, we interrogated this mutation in the context of FGF10's protein sequence and three-dimensional structure, and followed the subcellular fate of tagged proteins containing this or other combinatorial FGF10 mutations, in vitro. We report that FGF10 harbours two putative nuclear localization sequences, termed NLS1 and NLS2, which individually or co-operatively promote nuclear translocation of FGF10. Furthermore, FGF10 localizes to a subset of dense fibrillar components of the nucleolus. G138E falls within NLS1 and abrogates FGF10's nuclear translocation whilst attenuating its progression along the secretory pathway. Our findings suggest that in addition to its paracrine roles, FGF10 may normally play intracrine role/s within FGF10-producing cells. Thus, G138E may disrupt both paracrine and intracrine function/s of FGF10 through attenuated secretion and nuclear translocation, respectively.

## **SUMMARY**

G138E, a LADD-syndrome causing FGF10 mutation, falls within a putative NLS motif and disrupts FGF10's nuclear trafficking as well as secretion. G138E may reduce the bioavailability of FGF10 for intracrine function/s within FGF10-producing cells and paracrine signalling in FGF10-responsive cells.

## INTRODUCTION

LADD (OMIM 149730) and ALSG (OMIM 180920) are rare autosomal dominant syndromes caused by a spectrum of heterozygous missense mutations in FGF10 and FGF-Receptor 2 (FGFR2) genes [1-4](Table 1). These syndromes are characterised by defects in tear and saliva production, accompanied by subtle craniofacial, limb, pulmonary and urogenital abnormalities, complementary to milder phenotypes observed in mice that are heterozygous for FGF10 or its cognate receptor, FGFR2-IIIb [5, 6]. Structural modelling and biochemical studies have attributed the human defects to impaired FGF10-FGFR2-IIIb interaction, or production of unstable proteins [7] (Table 1). Three of the FGF10 mutations occur outside its receptor-interacting interface, with two of these (W169X and K137X) predicted to generate a truncated non-functional protein (Table 1). However, the mechanism by which the third mutation – a Glycine (G) to Glutamic Acid (E) substitution at residue 138 - causes LADD [4] is unknown, and its apparent lack of involvement in receptor binding has raised the interesting possibility that FGF10 functions in multiple ways.

Fibroblast growth factors (FGFs) are a 22-member strong family of 17-34 kDa proteins with critical roles in embryonic and adult tissue growth and homeostasis [8]. FGFs have been classified into subfamilies according to peptide sequence homology, shared biochemical properties and biological functions. Most FGFs are secreted ligands, signalling through one of four tyrosine kinase trans-membrane FGFRs, in cooperation with sulphated proteoglycans. FGF-FGFR binding specificity is determined in part by alternative splicing of exons encoding FGFRs' third Immunoglobulin-like domains, yielding the so-called 'IIIb' and IIIc' isoforms.

Moreover, paracrine signalling and functionality is determined by tissue-specific and mutually exclusive expression of FGF ligands and their corresponding receptors. Typically, FGF10 is secreted by mesenchymal cells to regulate epithelial cell growth and branching morphogenesis by activating the epithelially-expressed FGFR2-IIIb isoform [9-11].

In addition to their paracrine signalling role, several FGFs are thought to function cell-autonomously, via intracellular partnership with scaffolding proteins [12]; receptor and non-receptor mediated re-uptake into cells [13]; interaction with FGFRs within endosomes [14]; and translocation into the nucleus/ nucleolus [15]. In some FGFs, this functional diversity is achieved via the generation and differential targeting of low versus high molecular weight (HMW) isoforms. For example, HMW FGF2 translocates to the nucleus to stimulate cell proliferation and negatively regulate bone mineralization [16, 17]. In contrast, nuclear FGF3 inhibits cell proliferation [18].

Since the LADD-causing G138E mutation lies outside the FGF10-FGFR2 interaction interface, in this study we sought alternative explanation/s for its loss-of-function effects. Using bioinformatics, structural modelling, site-directed mutagenesis and intracellular trafficking analysis, we show that FGF10 harbours two putative nuclear localization sequences (NLS), with G138E falling within one of these. In contrast to the wild type, rat proteins bearing the equivalent mutation (G145E), or compound mutations in a second putative NLS site, fail to traffic into the nucleus and become hyper-glycosylated in the cytoplasm. Moreover, G145E fails to progress through the intracellular secretory pathway, and transient overexpression of wild type or FGF10 mutant proteins inhibit mesenchymal cell proliferation and differentiation in vitro. Our results suggest that nuclear trafficking promoted by two putative NLS motifs may be

an important aspect of FGF10 functionality. Hence, G138E mutation may work by reducing the bioavailability of FGF10 at two levels – as a secreted form to FGF10-responding cells, and as a nuclear form within FGF10-producing cells themselves.

## **Material and METHODS**

### **Bioinformatics analysis**

Primary protein sequences were obtained from UniProt database and sequence alignments were performed using ClustalW2. Protein 3D models were constructed in Chimera 1.9 using RCSB Protein Data Bank files (1nun). The search for NLS sequences was performed on rat and mouse FGF10 sequences using NLStradamus and NucPred software tools (Suppl. Fig. 1), freely available online.

### **Cloning and generation of mutant constructs**

Using the appropriate restriction enzyme or HA tag encoding primers, a C-terminus HA-tagged FGF10 construct (FGF10-HA) was generated by PCR from a template plasmid encoding rat FGF10 cDNA (gift of Prof. Saverio Bellusci). These were scanned for undesirable mutations by Sanger sequencing before cloning as an EcoRI-NotI fragment into a mammalian expression vector, pN1, replacing an existing mCherry encoding fragment (Suppl. Fig. 2A; Clontech Laboratories Inc.). All point mutation-bearing FGF10 inserts (i.e. R/K to T substitutions) were generated by PCR using a QuikChange Lightning Site-Directed Mutagenesis Kit (Agilent Technologies), and the relevant custom designed mutation-bearing primers (Suppl. Fig. 2B). At the end of each reaction, residual WT FGF10-HA template was cleaved by DpnI

restriction digest, and the desired mutation-bearing products were selected by Sanger sequencing.

### **Cell cultures and plasmid transfections**

Human retinal pigment epithelial (ARPE19) and embryonic kidney (293T) cells were maintained in DMEM/F12 HAMS supplemented with 10% Foetal Bovine Serum (FBS; Invitrogen), respectively, supplemented with 0.1% gentamycin or 1% penicillin/streptomycin and 1% GlutaMAX (Gibco). ATDC5 cells were grown in DMEM/F12 HAMS (Gibco 21331) supplemented with 5% FBS; 1% penicillin/streptomycin; 1% GlutaMAX; 30 nM sodium selenite and 10 µg/ml human Transferrin. Primary brain cultures were established by enzymatic digest and dissociation of freshly isolated hypothalamus from brains of 3-6 weeks old wild type mice. Hypothalamic cells were then grown as a monolayer in DMEM/F12 HAMS (Gibco 21331) supplemented with 5% FBS; 1% penicillin/streptomycin; 1% GlutaMAX; B27 Supplement (Gibco); 35 µg/ml bovine pituitary extract (Invitrogen) and 20 ng/ml each of EGF and FGF2 (Peprotech). For transient transfections, cells were seeded at 10 to 40x10<sup>3</sup> on poly-D-lysine (20µg/ml) coated glass coverslips placed in a 12- or 24-well plate. At 80% confluency, cells were transfected for four hours using JetPrime Reagent (Polyplus transfections) allowing 1 part DNA to 2 Parts JetPrime, aiming for 1µg of plasmid DNA per well. At 24h, 48h or 72h post transfection, cells were fixed for 15 minute in a 4% paraformaldehyde (PFA; pH 7.4) solution.

### **Immunohistochemistry, Microscopy and Imaging**

In preparation for immunolabelling, PFA-fixed cells were treated with 1% NP-40 and blocked in 10% Normal Goat Serum (NGS) solution for 1 hour at room temperature,

before overnight incubation at 4°C with primary antibodies diluted in 0.2% NGS/PBS. These were: Mouse anti-HA (1:1000; Cell Signalling); Rat anti-BrdU (1:1000; Thermo Scientific PA5-33256); Rabbit anti-TGN46, ERP60 and  $\beta$ COP (1:500 each; kind gift of Prof T. Wileman and Dr. P. Powell); and Rabbit anti-Fibrillarin (1:1000; Abcam). Cells were washed 3-5 times in 0.2% NGS/PBS and the relevant species-specific secondary antibodies conjugated to Alexa488 or Alexa568 (1:1000) were applied for 1h at room temperature. Coverslips carrying immunolabelled cells were mounted onto glass slides using Vectashield mounting medium (Vector Labs) and visualised using a Zeiss Axioplan2 microscope, with or without an Apotome attachment, under identical optical threshold settings. Images were acquired and processed using Axiovision 4.8 and ImageJ softwares. A typical experiment (per construct) was comprised of transfecting two coverslips and taking measurements from ten random areas ie, five from each coverslip. Within each photographed area, total cell number (ranging from 60-110 cells per area) as well as the proportion of transfected cells was determined, with the latter comprising about 20-30% of the total. The pattern of HA localization in each transfected cell was classified into three categories: exclusively or predominately nuclear; exclusively or predominantly cytoplasmic; and equal cytoplasmic and nuclear distribution.

The degree of HA-tag and secretory pathway marker colocalization was measured using Volocity 6.3 software. Briefly, 10 randomly selected fluorescent cells from each immunolabelling combination were photographed under the relevant channels - red (Alexa 568) for HA and green (Alexa 488) for secretory pathway markers (either ERp60,  $\beta$ COP or TGN46). After setting the appropriate thresholds, a scatter plot of co-localising markers was generated, from which Pearson's Correlation coefficient ( $R_r$ ) was calculated. Values range from -1.0 to 1.0, where values above 0.5 signify

co-localisation, and values below 0.5 indicate negative or no significant correlation between markers.

### **Subcellular Fractionation**

Cell fractionation (cytoplasmic versus nuclear) was carried out following the protocol of Dimauro et al. [19]. In brief, 24 hours post transfection, 293T cells were washed in cold PBS, and pelleted. Cytoplasmic fraction was extracted by treating cells with STM buffer (250 mM sucrose; 50 mM Tris-HCl pH 7.4; 5 mM MgCl<sub>2</sub>) in the presence of 1% Halt protease inhibitor cocktail (Thermo Fisher Scientific). Cells were then washed in STM buffer, precipitated in pre-cooled acetone and re-suspended in STM buffer. The nuclear fraction was extracted in NET buffer (20 mM HEPES pH 7.9; 1.5 mM MgCl<sub>2</sub>; 0.5 M NaCl; 0.2 mM EDTA; 20% glycerol; and 1% TritonX-100) in the presence of 1% Halt cocktail, incubated on ice for 45 min and centrifuged at 9000 *xg* to remove debris.

### **Western Immunoblotting**

ARPE cells cultured on 10cm petri dishes were transfected with 3µg of relevant plasmids, and 24 hours later lysed in ice-cold modified RIPA buffer (150mM NaCl; 50mM Tris; 1.25mM EDTA; 1% Triton, 1% sodium deoxycholate; and 0.1% SDS) containing protease inhibitors. Total protein concentration was determined using a BCA assay kit (Thermo Fisher Scientific) and cell lysates were stored at -20°C until use. Protein lysate was subjected to SDS/PAGE, electrophoretic semi-dry transfer to nitrocellulose membranes, and incubated with primary mouse antibodies against β-actin (1:1000) and HA (1:1000; Cell Signalling) at 4°C for 24h. Subsequently, HRP-conjugated goat-anti-mouse antibodies were applied (1:1000) and membranes were

incubated in ECL solution (100mM Tris pH8; 1.25mM luminol; 0.2 mM coumaric acid; and 0.01% H<sub>2</sub>O<sub>2</sub>) and exposed to Hyperfilm ECL (for 5-30 seconds for  $\beta$ -actin; 15 minutes for HA).

### **Cell Proliferation assays**

20 hour post-transfection with the relevant constructs, ATDC5 cells were pulsed with 3 $\mu$ g/ml BrdU for 4 hours, fixed in 4% PFA, and treated with 1M HCl at 47°C for 30min before sequential immunolabelling with mouse anti-HA and rat anti-BrdU antibodies and the relevant fluorophore-tagged secondary antibodies. One hundred cells expressing HA were examined for expression of BrdU. The experiment was repeated three times on different occasions, using cells of similar passage number.

### **ATDC5 cell differentiation assays**

ATDC5 cells were grown to 90% confluency in 24-well plates. To induce differentiation, growth medium was supplemented with 50  $\mu$ g/ml ascorbic acid (Sigma) and Insulin-Transferrin-Selenium solution ITS-G (Gibco, 1:100 dilution). Cells were transfected three times, first on the day of differentiation and every two days thereafter, with HA-tagged constructs or a control pmCherry-N1 vector. Some cells were additionally treated with 10ng/ml FGF10 (Peprotech). Differentiated mesenchymal condensations/ nodules normally appeared within 14 days. After 16 days in culture, cells were fixed for 10 min with 4% paraformaldehyde at RT, and treated for 5 min at -20°C with pre-chilled absolute methanol. Differentiated cells were revealed by 30 min staining with 0.5% Alcian blue in 0.1M HCl at RT. After photographing the stained cells, Alcian blue was extracted by a 6-hour incubation at RT with 6M guanidine hydrochloride, and quantified using a spectrophotometer at 630nm. Each treatment was replicated 4 times.

### **Detection of Fgf10 and FGF-Receptor isoforms by standard Rt-PCR**

mRNA was isolated from HEK293T cells as well as differentiated undifferentiated ATDC5 cells using Trizol reagent, and subjected to Rt-PCR to detect Fgf10, the IIIb and IIIc isoforms of FGF-receptors 1-3 and FGFR4-IIIc, using previously described primers, protocols and cycle conditions [20, 21].

### **Statistical analysis**

Raw data was imported into and analysed by IBM SPSS Statistic 22 software.

Normally distributed data of equal variance were compared using Student's t Test (for two samples), or ANOVA post hoc Tukey (for greater than two samples).

## RESULTS

### Putative Nuclear Localisation Sequences within FGF10

To investigate the mode/s of G145E function, we considered a potential intracellular mechanism involving nuclear trafficking. Active nuclear import of proteins requires nuclear localization sequence (NLS) motif/s, typically composed of a short stretch of positively charged amino acids such as arginine and lysine. NLS motifs can occur anywhere within a protein sequence, but must be exposed at the surface to allow for interaction with adaptor proteins such as importin- $\alpha$  and  $\beta$ -Kap, which facilitate protein trafficking through the nuclear pore complex [22].

Using two independent software algorithms, NLStradamus [23] and NucPred [24] we identified a putative NLS motif encoded by amino acids 194 to 202 (RRGQKTRRK). This is in addition to a more N-terminal NLS-like sequence (rat residues 142NKKGKLY148) noted by Kosman et al. [25] resembling, but not homologous to, a putative NLS found in FGF1 (i.e YKKPKLL). Here on we term these NLS2 and NLS1, respectively (Fig. 1; Suppl. Fig. 1A,B). Sequence alignments revealed that both NLS1 and NLS2 are fully conserved between rat, mouse and human, and show high conservation amongst other vertebrates (Fig. 1A). Moreover, 3D-modelling showed that both motifs are exposed and reside away from the FGF10-FGFR2 interaction interface (Fig. 1B). Strikingly, the LADD-type G138E falls within NLS1, and the G138 residue (rat G145) is not only conserved among different mammalian species (Fig. 1A) but also across different FGF family members (Suppl. Fig. 1C,D). To understand the significance of this high conservation, we scrutinized structural models of FGF10 and found that G145 interacts via a single H-bond with residue 196 (G196) of NLS2. Furthermore, side chains of the basic residues within NLS2 extend away from the

protein surface (Fig. 1C) allowing for potential contacts and interactions with other molecules, such as importins. Combined, these analyses suggested that NLS1 and NLS2 may function individually or co-operatively to promote nuclear import of endogenous FGF10.

### **Glycine 145 is critical for nuclear translocation of FGF10**

To test the idea that FGF10 can translocate into the nucleus, we first analysed its cellular distribution. In the absence of commercial antibodies to specifically detect endogenously produced FGF10 by immunocytochemistry (our unpublished investigations), we followed the fate of FGF10 molecules tagged at their C-terminus with Haemagglutinin A (FGF10-HA). The relevant construct was generated by PCR from rat cDNA and cloned into pN1 mammalian expression vector (Addgene; Suppl. Fig. 2A). ARPE (retinal pigment epithelial) cells were transiently transfected with the corresponding vector and FGF10-HA was detected by anti-HA immunolabelling, at 24, 48 and 72 hours post transfection. Although a variety of cellular HA distributions were observed, consistently in 20-25% of transfected cells, HA was predominantly nuclear, regardless of time-point analysed (Fig. 2A,B). This was not peculiar to ARPE cells, as similar extent of nuclear HA localization were found in transfected ATDC5 (chondrogenic mesenchymal) cells; primary adult mouse hypothalamic cells and HEK293T cells (Fig. 2A,B; data not shown). Moreover, a similar pattern and proportion of nuclear FGF10-HA was observed after transfection of serum-starved growth arrested cells, suggesting that its nuclear localization is not dependent on nuclear membrane breakdown during M phase (Fig. 2C; data not shown). On closer examination, some cells exhibited discrete nucleolar FGF10-HA localization (see

also below). Generation of Fgf10 transcripts from transfected plasmids was confirmed by real time Rt-PCR (data not shown).

Because LADD-causing G138E falls within a putative NLS (NLS1), next we asked whether introducing the mutant protein into cultured cells affects its nuclear localization. Thus, a corresponding C-terminus HA-tagged rat G145E construct was generated through site-directed mutagenesis (Suppl. Fig. 2), transfected into ARPE cells, and analysed as described for wild type FGF10-HA. Generation of G145E-encoding transcripts was also confirmed by real time Rt-PCR (data not shown). Remarkably, in all cell types and at all time points examined, G145E-HA was excluded from the nucleus and restricted to the cytoplasm (Fig. 2A,B).

A glutamic acid substitution at residue 145 would create an acidic side chain, potentially disrupting the interaction of FGF10 with importins. On the other hand, a glycine residue *per se* could be critical for the nuclear translocation. To distinguish between these possibilities we also analysed the cellular distribution of HA-tagged G145V and G145A FGF10 constructs, choosing valine (V) or alanine (A) residue substitutions to mimic the small size of the glycine residue. However, both G145V-HA and G145A-HA molecules behaved like G145E-HA and showed nuclear exclusion (Suppl. Fig. 3A-D'; data not shown).

These findings show that nuclear translocation of FGF10 can occur in multiple cell types – at least following its cytoplasmic introduction in our experimental settings. Furthermore, a G138E LADD-type amino acid substitution can disrupt this trafficking and a glycine residue at position 138 (rat 145) is critical for this process.

### **Distinct NLS2 residues are also important for FGF10 nuclear trafficking**

To determine the functionality and key elements of the NLS2 that may be important for nuclear translocation of FGF10, six basic residues (lysine and arginine) at positions 194, 195, 198, 200, 201 and 202 were individually mutated to a neutral threonine (T) using site directed mutagenesis (Fig. 3A; Suppl. Fig. 2B). In anticipation that mutagenesis of single NLS2 residues may not suffice – as observed in other NLS-bearing FGFs [26, 27], we also generated three double-mutants (R194T/R195T, R200T/R201T and R200T/K202T) and a single quadruple-mutant construct (R194T/R195T/R200T/K202T, here on termed 4T-NLS2), all tagged with HA at their C-termini (Fig. 3A). These were transfected into ARPE cells and subcellular distribution of HA was monitored by immunolabelling alongside sister cultures transfected with FGF10-HA or G145E-HA mutant.

We found that in contrast to G145E (NLS1), single residue substitutions in NLS2 had no significant impact on nuclear translocation of FGF10. However, double mutations significantly altered the balance of subcellular localization in favour of the cytoplasm, and the quadruple mutation (4T-NLS2) mimicked the effect of G145E, excluding FGF10 from the cell nucleus altogether (Fig. 3B-D). This was verified by immunolabelling of transfected cells, or by immunoprobings their nuclear and cytoplasmic protein sub-fractions with antibodies against fibrillarin, a ribonucleolar protein, and GAPDH, a cytoplasmically-restricted protein, in combination with HA (Fig. 4). First, FGF10-HA clearly co-localised with a subset of dense fibrillar components (DFC) found in the nucleolus (Fig. 4A). Second, when compared to wild type FGF10, G145E and 4T-NLS appeared more abundant in the cytoplasmic fraction (Fig. 4B). Interestingly, wild type FGF10 accumulates largely as its mature 21kDa form within the nucleus, whilst the cytoplasmic fraction additionally contains its 25kDa immature species (see below).

Since mutation of NLS2 mimics the effects of G145E mutation in NLS1, these findings suggest a distinct cluster of NL2 residues are also important for FGF10's nuclear trafficking, possibly acting independently or through a conformational association with NLS1.

### **Nuclear-excluded FGF10 mutants undergo hyperglycosylation and disrupt FGF10's secretory pathway**

To assess the molecular consequence of mutations that induce nuclear exclusion, whole cell lysates from ARPE cells transfected with wild type or mutant HA-tagged constructs were isolated, resolved by SDS page and probed with anti-HA antibodies. The efficacy of anti-HA antibodies in these assays was verified using a control vector encoding HA-tagged SMAD2, detectable as a 55 kDa product (Fig. 5A).

Wild type FGF10 is normally detected as a full-length 25kDa product as well as a mature 21kDa protein lacking the signal peptide, required for progression through the secretory pathway [28, 29]. Here, the 21kDa band was detected in all samples except for G145E and G145V (Fig. 5A). In contrast, a novel strong 30kDa species was present in the G145E and G145V samples as well as R200T/K202T and 4T-NLS2, but not in R194/R195T, R194T, K198T single mutants or wild type. We also noted that the 25kDa product was generally stronger whenever the 30kDa protein was present (Fig. 5A). Based on its size and the reduced conditions of SDS page, we posit that the 30kDa product is an unlikely product of intracellular ligand-ligand dimerization (>50 kDa) or ligand-FGFR partnership (>110 kDa). Since secreted FGFs can be glycosylated at multiple positions and FGF10 is predicted to carry at least 26 potential sites (Fig. 5B), we investigated the possibility that the 30kDa species represents a hyperglycosylated form of FGF10. Cell lysates containing

FGF10-HA, G145E-HA and a selection of single and double mutants as well as the 4T-NLS2 were subjected to 'N' deglycosylation with PNGase F, or to deglycosylation with a cocktail of 'O and N' deglycosylating enzymes. As shown in Fig. 5C, N-deglycosylation alone was sufficient to reduce not only the 30kDa, but also the 25kDa products in all samples, to a single 21kDa product. This suggests that 'O' glycosylation of FGF10 in cultured cells is minimal.

A likely interpretation of these findings is that whilst abolishing nuclear translocation, the LADD-type G145E traps the mutant protein in the cytoplasm, permitting its hyperglycosylation with a possible deleterious effect on its secretion. Unfortunately, low transfection levels did not permit isolation of sufficient secreted protein from the culture media in order to compare the secretory potential of wild type versus mutant FGF10, although poor FGF10 secretion from transfected cells has been noted by others [29]. Therefore, as an alternative approach we compared the cytoplasmic progression of wild type and G145E along the secretory pathway.

### **G145E mutant protein accumulates within the Endoplasmic Reticulum**

To examine progression through the secretory pathway, we compared the distribution of FGF10-HA, G145E-HA and 4T-NLS2-HA in three subcellular compartments that define the successive stages of secretion. Thus, transfected cells were co-immunolabelled with anti-HA as well as antibodies against ERp60, an early secretory pathway chaperone within ER;  $\beta$ COP, a marker of transport between ER and Golgi; and TGN46, demarcating Golgi and vesicle transport stages (Schematic, Fig. 6A). Close scrutiny of high resolution images from randomly selected cells showed that whilst FGF10-HA colocalised with all three markers (Fig. 6B,C,F,I), expression of G145E-HA was restricted to the ERp60-positive compartment (Fig.

6B,D,G,J), and 4T-NLS2 showed a much weaker phenotype (Fig. 6B,E,H,K). In agreement with whole cell lysate analysis (Fig. 5A), these results suggest that the G145E mutant protein fails to progress through the secretory pathway. However, the causal relationship between nuclear exclusion, hyperglycosylation and secretion cannot be wholly ascertained from our experimental approach.

### **Proliferation and differentiation of ATDC5 cells is differentially affected by mis-expression or exogenous treatment with FGF10**

An important function of FGF10 is to regulate the formation and patterning of cartilage in vivo [30, 31]. To test whether the perturbation of cellular trafficking reported above impacts cell behaviour in vitro, we measured the rate of cell proliferation and differentiation in ATDC5 cells – a chondrogenic mesenchymal cell line which expresses transcripts for FGF10 and FGFR2-IIIc, and to a lesser degree, FGFR1-IIIc, FGFR2-IIIb and FGFR3-IIIc, but not FGFR1-IIIb (Rt-PCR data; not shown). Sister cultures of ATDC5 cells transfected with constructs encoding HA-tagged wild type FGF10, G145E- or 4T-NLS2-bearing mutations, or a control mCherry vector, were BrdU-pulsed for 4 hours and then immediately analysed for co-expression of BrdU with mCherry or HA. Compared to mCherry-transfected cells, all FGF10-bearing constructs showed a significant reduction in cell proliferation, but no significant differences were noted between wild type and mutant constructs (Fig. 7A-C). Similarly, the level of chemically-induced differentiation of ATDC5 cells into Alcian-blue-positive chondrocytes was significantly lower in cells transfected with FGF10-carrying constructs, when compared to non-transfected or mCherry transfected cultures, with no marked difference between different FGF10-carrying constructs (Fig. 7D-J). Separately, we also measured the rate of differentiation of

non-transfected ATDC5 cells in response to exogenously applied FGF10 (R&D systems; concentration ranges 1, 10 or 100 ng/ml). No discernable effect on cell differentiation was noted at 1 or 100 ng/ml, but a higher level of cell death was evident at 100ng/ml. However, and in contrast to FGF10 transfections, 10ng/ml of exogenous FGF10 promoted ATDC5 cell differentiation, and, supplementation of FGF10-HA transfected cultures with exogenous FGF10 partially rescued the inhibitory effects of FGF10-HA (Fig. 7I,I' and J; data not shown).

In sum, although abrogation of nuclear trafficking does not yield a unique effect, over-expression of FGF10, whether wild type or mutant, does perturb the proliferation and differentiation of mesenchymal cells in the paradigms tested. This suggests that in ATDC5 cells FGF10 may have multiple cell-intrinsic modes of action - nuclear and/or non-nuclear. Nonetheless, the contrasting effects brought about by FGF10 transfection vs exogenous FGF10 treatment, indicates that the cell-autonomous function/s of transfected constructs are unlikely to involve cell surface exposed FGFRs.

## **DISCUSSION**

ALSG and LADD syndromes are commonly caused by heterozygous mutations in FGF10 or its cognate receptor FGFR2-IIIb, affecting tissues that develop and function through epithelial-mesenchymal cross talk, utilising this signalling pathway. Most FGF10 mutations are postulated to yield proteins that are truncated, unstable, or defective in receptor interactions, explaining their partial loss-of-function effects (Table 1). However, the functioning of a FGF10 G138E residue substitution has remained enigmatic. In this study, we analysed this mutation *in silico* and modelled the equivalent rat protein (G145E) *in vitro*. Although we cannot exclude the possibility that G138E encodes an unstable protein targeted for rapid degradation *in vivo*, our results rather suggest that falling within a putative NLS sequence, G145E works by attenuating the process of FGF10 secretion, coupled to a novel nuclear trafficking role. The latter is supported by the identification of a second putative NLS sequence within FGF10, the mutation of which also abrogates FGF10 nuclear localization. We propose therefore that the G138E pathology may involve two cellular compartments and multiple biological processes *ie.* attenuation of paracrine signalling in epithelial cells secondary to reduced FGF10 secretion by mesenchymal cells, as well as perturbed cell-autonomous FGF10 function/s in mesenchymal cells themselves (summarised schematically in Suppl. Figure 7).

### **Nuclear translocation of FGF10 and its putative functions**

As a 21-25 kDa protein, FGF10 is in principle small enough to passively traffic in and out of the nuclear pore complex and attain an equal nuclear/ cytoplasmic cell distribution at any given time. However, we found that most transiently transfected cells exhibit predominantly cytoplasmic or nuclear FGF10 as late as 72 hours post

transfection, suggesting that FGF10 is actively compartmentalized and/or retained within the cell nucleus. This phenomenon is not a peculiarity of our transfection system since Kosman et al [25] showed that exogenously applied FGF10 can enter the cell nucleus, possibly in association with FGFRs. They also reported that mutagenesis of basic residues flanking G145 in NLS1 can diminish, but not abrogate, this route of nuclear localization. By contrast, we showed that the mutation of the evolutionary conserved glycine 145 alone abrogates both FGF10's nuclear localization and progression along the secretory pathway. It may be that the basic residues of NLS1 have a dual function of binding FGFRs and promoting nuclear entry. Interestingly, an arginine 187 to valine substitution in mouse NLS2 (Rat R194V) alters FGF10's extracellular receptor binding dynamics and converts it to an FGF7-like molecule in branching morphogenesis assays [32]. In our assays, mutation of R194 alone (to threonine) did not affect the normal rate of FGF10 nuclear trafficking, perturbing this function only in combination with other mutations in NLS2.

Dynamics and mechanisms of nuclear translocation notwithstanding, the significance and role of nuclear-targeted FGF10 molecules remains unknown. We showed that FGF10 becomes localized to a subset of dense fibrillar components of the nucleolus, demarcated by the expression of Fibrillarin. The nucleolus is important for the generation and assembly ribosomal RNA as well as non-coding RNAs involved in pre-mRNA splicing and protein synthesis, and, formation of RNA-telomerase complexes [33]. Hence, it is tempting to speculate that by associating with the molecular machinery of the nucleolus, FGF10 participates in one or more of the above processes to regulate gene expression or cell cycle control, akin to roles ascribed to nucleolar FGF2 and FGF3. Nucleolar FGF2 directly regulates synthesis

of ribosomal RNA and stimulates Polymerase I transcription through binding to UBF transcription factor [34]. Nucleolar FGF3 is postulated to inhibit cell proliferation by binding to NoBP protein [35].

Targeting of FGF10 to the nucleus could also play a critical stoichiometric role in regulating the normal level of paracrine FGF10 signalling. Numerous studies show that the level of FGFR signalling is exquisitely regulated and is critical for multiple biological outcomes during normal development as well as pathological conditions [10]. A key factor in this process is the quantity and bioavailability of FGF ligands. For example, FGF10 is a driver of hyperactive FGFR2 mutations that cause Apert syndrome, and its genetic knockdown in a mouse model of Apert syndrome rescues much of the related defects [36]. Hence, the amount of secreted FGF10, available for paracrine signalling in epithelial cells, may normally be determined by titration against its nuclear-targeted forms in mesenchymal cells.

A potential cell autonomous role for FGF10 within FGF10-expressing cells themselves, whether nuclear or otherwise, gains credence from the discovery of tissues wherein FGF10 is unconventionally expressed in the epithelial cell compartment, or, from which FGF10's cognate receptor, FGFR2-IIIb is absent. Notably, FGF10 is atypically expressed in the developing Otic epithelium [37] where it regulates cell specification, in contrast to its paracrine regulation of cell proliferation or differentiation. Interestingly, a significant number of LADD syndrome patients suffer from hearing defects [1]. In the adult brain (hypothalamus), expression of FGF10 by a population of neural stem cells termed tanycytes, is not complemented by FGFR2-IIIb or FGFR1-IIIb expression, where the IIIc isoforms of FGFRs 1-3 predominate. Tanycytes produce new appetite/energy balance regulating neurons in

vivo [38] and we showed that FGF10 can translocate into the nucleus of these cells in vitro (Fig. 1A). Thus, it would be interesting to investigate whether partial-loss-of FGF10 function in LADD/ALSG patients perturbs the homeostatic functions of hypothalamus, such as energy expenditure.

In summary, our in vitro investigations of a LADD-syndrome FGF10 point mutation has led us to postulate novel mechanisms involving defects in secretion linked to nuclear translocation of FGF10. This may not be a common mode of function in all LADD/ALSG mutations, as evidenced by the diversity and varying degrees of phenotypic penetrance in these patients. Nonetheless our results highlight another potential level of complexity in FGF10 biology during normal development and in disease, warranting further investigations using inducible constructs to fine dissect the intermediate steps of FGF10 trafficking, or in vivo modelling of distinct LADD mutations in transgenic animal models to test the differential role of individual mutations.

## Table and figure legends

### Table 1. Spectrum of LADD/ALSG syndrome causative mutations

Current spectrum of mutations in FGF10 or FGFR2-IIIb that results in ALSG and LADD syndromes, with their predicted or characterised molecular properties. Star (\*) denotes FGF10 mutations occurring outside its cognate receptor's binding site. To date, the mode of action for a G138E mutation (rodent equivalent, G145E) has remained unknown. A rare FGFR3 mutation has also been described [2].

### Figure 1. Structure, conservation and positioning of two putative NLS motifs in FGF10

A) Amino acids encoding putative NLS1 (green) and NLS2 (Red) in FGF10 show a high degree of conservation from fish to mammals. B) Three dimensional modelling viewed from two angles to show close proximity of NLS1 (green) and NLS2 (red) motifs and their surface exposure away from FGF10's (light brown) interaction interface with FGFR2-IIIb (blue). C) Capacity for a direct hydrogen bond (blue line) between carboxyl oxygen of G145 residue in NLS1 (purple) and amide hydrogen of G196 in NLS2, and, lateral protrusion of NLS2 basic residues (R194, R195, K198, R200, R201 and K202) away from FGF10 molecule.

### Figure 2. LADD-type G145E mutation inhibits the normal nuclear trafficking of FGF10

A) Transiently transfected HA-tagged FGF10 is found in both the cytoplasm and nucleus of multiple cell types, whereas an HA-tagged G145E mutant is absent from cell nucleus. Images, 24 hours post transfection. B) Temporal quantification of nuclear/ cytoplasmic localisation shows a time-independent difference between FGF10-HA and G145E in ARPE cells (Error bars – SE; ANOVA \*\*\*\*  $p \leq 0.0001$ ;  $n=3$ ). C) Nuclear translocation of FGF10-HA can occur in growth arrested ARPE cells. Scale bars: 50  $\mu\text{m}$  in A, 25  $\mu\text{m}$  in C.

**Figure 3. Combinatorial mutation of distinct residues in NLS2 mimic the nuclear exclusion effect of G145E in NLS1**

A) Single and combinatorial threonine (T) residue substitutions in NLS2, created by site-directed mutagenesis. B) Quantitative comparison of nuclear/ cytoplasmic localization of NLS2 mutants with wild type FGF10-HA and G145E mutant in ARPE cells (Error bars - SE; ANOVA \*\*\*\*  $p \leq 0.0001$ ;  $n=4$ ). C, D) Representative images of ARPE cells transfected with HA-tagged single or multiple NLS2 mutant constructs, demonstrating nuclear exclusion in a subset of these mutants, particularly 4T-NLS2 (quantified in B). Scale bars: 50  $\mu\text{m}$  in C and D.

**Figure 4. Association of FGF10-HA with cell nucleolus and molecular compartmentation of wild type and mutant FGF10 proteins**

A) Co-localisation of HA and a nucleolus-restricted protein, Fibrillarin, demonstrates clear association of FGF10-HA with a subset of nucleolar aggregates (arrows). B) Use of anti-Fibrillarin and GAPDH to compare molecular abundance of FGF10-HA,

G145E and 4T-NLS2 in cytoplasmic and nuclear fractions of transfected cells. A control m-Cherry construct, probed by anti-Ds-Red antibodies, is found in both fractions and no HA is found in non-transfected cells. Note, mutant proteins are relatively more abundant in the cytoplasmic fractions. Scale bar in A: 25  $\mu$ m.

### **Figure 5. NLS mutations perturb the molecular processing of FGF10**

A) Characteristics of HA-tagged WT and mutant FGF10 proteins, immunoprobed with anti-HA antibodies. A 25kDa full-length immature FGF10 protein is observed in all lanes, but the nuclear-excluded mutant forms (lanes 2, 3, 7 and 8) additionally show a 30kDa product. 21kDa signal-peptide lacking mature form of FGF10 fails to be produced by NLS1 mutants (lanes 2 and 3). Lane 9, positive control for HA; Lane 10, non-transfected control. B) Location of at least 26 potential glycosylation sites on rat FGF10 protein sequence: 'O'-linked in italics; 'N'-linked in bold. C) Treatment of WT and mutant proteins with de-glycosylating reagents abrogates the 30 and 25kDa products in favour of a 21kDa product.

### **Figure 6. Abnormal cytoplasmic retention and trans-Golgi trafficking of G145E and 4T-NLS molecules**

A) A schematic of the trans-Golgi secretion pathway and protein markers delineating its intermediate steps: ERp60 (early ER stage);  $\beta$ COP and TGN46 (late ER stages). B) Quantification of immuno-colocalisation between these markers and HA-tagged FGF10, G145E and 4T-NLS2 molecules (shown in panels C-K), using Pearson's Correlation coefficient (see methods). FGF10-HA and 4T-NLS2 show

values above 0.5, indicative of colocalisation with all three markers, whereas G145E co-localises only with the ERp60. C-K) ARPE cells transfected with FGF10-HA (C,F,I), G145E (D,G,J) and 4T-NLS2 (E,H,K), and probed with Trans-Golgi secretion pathway markers, showing that whilst the WT protein is processed through the pathway, the G145E is sequestered at the ER stage. Scale bars: 20  $\mu\text{m}$  in all panels.

### **Figure 7. Effects of FGF10 over-expression or exogenous treatment on ATDC5 cell proliferation and differentiation**

A-B') Examples of ATDC5 cells transiently transfected with FGF10-HA or a control mCherry construct, and pulsed with BrdU. C) Introduction of FGF10-HA or its mutant forms significantly reduces cell proliferation when compared to a control mCherry vector. (D-I') Representative low and high power images of ATDC5 cells induced to differentiate in 24-well plates without any transfection (D,D'), or after transfection with a mCherry control (E,E'); FGF10-HA and its mutant forms alone (F-H'); or FGF10-HA, in the presence of exogenous FGF10 (I,I'). Transfection with FGF10-HA or its mutant forms delays the differentiation of ATDC5 cells, evidenced by formation of fewer Alcian blue-positive nodules and lower spectrophotometric detection of Alcian blue (J). (I,I',J) Exogenously-applied FGF10 partially rescues the inhibitory effects of FGF10-HA transfection. Scale bars: 20  $\mu\text{m}$  in A; 1000  $\mu\text{m}$  in D,E,F,G,H and I; 100  $\mu\text{m}$  in D',E',F',G',H' and I'. (Error bars in C, J are SE; ANOVA \* $p\leq 0.05$ ; \*\* $p\leq 0.01$ , \*\*\* $p\leq 0.001$ , \*\*\*\* $p\leq 0.0001$ . C, n=5; J, n=4).

## Supplementary Figures

### Suppl. Figure 1. Bioinformatic analysis of putative NLS sequences in FGF10.

A, B) Use of NLStradamus and NucPred highlights a weak NLS (here termed NLS2) site in rat Fgf10 exon 3, encoded by amino acids 194 to 202 and conserved across species (Figure 1A). C, D) Full conservation of Glycine 145 residue in rat NLS1 within related FGF7 subfamily members (C), as well as different FGFs (D).

### Suppl. Figure 2. P-N1 cloning vector backbone and site-directed mutagenesis primers sequences.

A) Schematic diagram of pN1 mammalian expression vector carrying mCherry, used as control. HA-tagged WT or mutant FGF10 constructs were cloned into this vector as EcoRI-NotI tagged PCR fragments, replacing mCherry. B) Primer sequences used for HA and restriction enzyme tagging; PCR amplification of FGF10 from a rat cDNA plasmid (gift of Prof. Saverio Bellusci); and site-directed mutagenesis. Single base pair substitutions inducing site-directed mutagenesis are shown in bold (second row and rows below it).

### Suppl. Figure 3. Importance of Glycine residue 145 (rat) to FGF10's nuclear trafficking.

A, C) Structural modelling showing the substitution of glycine 145 in NLS1 with two larger amino acids, valine (A, A') or alanine (C, C'), coloured purple. B,D), Nuclear exclusion of both HA-tagged G145V (B, B') and HA-tagged G145A (D, D') FGF10

molecules in cultured cells (B,D), mimicking the G145E mutation. Scale bars: 20  $\mu\text{m}$  in panels B,D.

**Suppl. Figure 4. Putative modes of FGF10 function during normal development, and partial-loss-of function in LADD.**

A) FGF10 is produced mainly by mesenchymal cells and regulates epithelial cell biology through paracrine action. However, it may have important cell-intrinsic function/s within the cytoplasm of mesenchymal cells themselves or through translocation into their nucleus. B) The likes of G145E (Human G138E) mutations that occur outside FGF10-FGFR2IIIb interaction interface, may induce LADD by affecting both epithelial and mesenchymal cell biology. i.e. by reducing the level of FGF10 available for paracrine signalling, and abrogating FGF10's nuclear translocation within mesenchymal cells. As an engineered compound mutation, 4T-NLS would not occur naturally but nonetheless its effects partially mimic that of G145E to show the importance of putative NLS sequences within FGF10.

**Acknowledgments**

We thank Professors Saverio Bellusci (Giessen, Germany), Tom Wileman, Penny Powell, Andrew Chantry, Jelena Gavrilovic and Charles Brearley (UEA, Norwich) for sharing constructs and antibodies and critical reading of the manuscript; and Dr. Lee Wheldon for valuable input in early stages of this work. We apologise to colleagues whose work could not be cited due to space limitations.

**Declaration of interest**

The authors have no commercial interests or otherwise to declare

### **Funding**

MM was supported by a UEA Dean Studentship, and this work was supported by a BBSRC research grant (reference BB/L003406/1) to MKH.

### **Author contribution/s**

MKH conceived and planned the study, and prepared the manuscript. MM and TG contributed to the planning and conducted the experimental work.

## References:

- 1 J. M. Milunsky, G. Zhao, T. A. Maher, R. Colby and D. B. Everman. (2006) LADD syndrome is caused by FGF10 mutations. *Clin Genet.* 69, 349-354.
  
- 2 E. Rohmann, H. G. Brunner, H. Kayserili, O. Uyguner, G. Nurnberg, E. D. Lew, A. Dobbie, V. P. Eswarakumar, A. Uzumcu, M. Ulubil-Emeroglu, J. G. Leroy, Y. Li, C. Becker, K. Lehnerdt, C. W. Cremers, M. Yuksel-Apak, P. Nurnberg, C. Kubisch, J. Schlessinger, H. van Bokhoven and B. Wollnik. (2006) Mutations in different components of FGF signaling in LADD syndrome. *Nat Genet.* 38, 414-417.
  
- 3 D. B. Chapman, V. Shashi and D. J. Kirse. (2009) Case report: aplasia of the lacrimal and major salivary glands (ALSG). *Int J Pediatr Otorhinolaryngol.* 73, 899-901.
  
- 4 M. Entesarian, J. Dahlqvist, V. Shashi, C. S. Stanley, B. Falahat, W. Reardon and N. Dahl. (2007) FGF10 missense mutations in aplasia of lacrimal and salivary glands (ALSG). *Eur J Hum Genet.* 15, 379-382.
  
- 5 H. Min, D. M. Danilenko, S. A. Scully, B. Bolon, B. D. Ring, J. E. Tarpley, M. DeRose and W. S. Simonet. (1998) Fgf-10 is required for both limb and lung development and exhibits striking functional similarity to *Drosophila* branchless. *Genes Dev.* 12, 3156-3161.

- 6 L. De Moerlooze, B. Spencer-Dene, J. Revest, M. Hajihosseini, I. Rosewell and C. Dickson. (2000) An important role for the IIIb isoform of fibroblast growth factor receptor 2 (FGFR2) in mesenchymal-epithelial signalling during mouse organogenesis. *Development*. 127, 483-492.
- 7 I. Shams, E. Rohmann, V. P. Eswarakumar, E. D. Lew, S. Yuzawa, B. Wollnik, J. Schlessinger and I. Lax. (2007) Lacrimo-auriculo-dento-digital syndrome is caused by reduced activity of the fibroblast growth factor 10 (FGF10)-FGF receptor 2 signaling pathway. *Mol Cell Biol*. 27, 6903-6912.
- 8 D. M. Ornitz and N. Itoh. (2015) The Fibroblast Growth Factor signaling pathway. *Wiley Interdiscip Rev Dev Biol*. 4, 215-266.
- 9 X. Zhang, O. A. Ibrahimi, S. K. Olsen, H. Umemori, M. Mohammadi and D. M. Ornitz. (2006) Receptor specificity of the fibroblast growth factor family. The complete mammalian FGF family. *J Biol Chem*. 281, 15694-15700.
- 10 M. K. Hajihosseini. (2008) Fibroblast growth factor signaling in cranial suture development and pathogenesis. *Frontiers of oral biology*. 12, 160-177.
- 11 N. Turner and R. Grose. (2010) Fibroblast growth factor signalling: from development to cancer. *Nat Rev Cancer*. 10, 116-129.

- 12 Q. F. Wu, L. Yang, S. Li, Q. Wang, X. B. Yuan, X. Gao, L. Bao and X. Zhang. (2012) Fibroblast growth factor 13 is a microtubule-stabilizing protein regulating neuronal polarization and migration. *Cell*. 149, 1549-1564.
- 13 S. J. Coleman, A. M. Chioni, M. Ghallab, R. K. Anderson, N. R. Lemoine, H. M. Kocher and R. P. Grose. (2014) Nuclear translocation of FGFR1 and FGF2 in pancreatic stellate cells facilitates pancreatic cancer cell invasion. *EMBO Mol Med*. 6, 467-481.
- 14 E. M. Haugsten, V. Sorensen, A. Brech, S. Olsnes and J. Wesche. (2005) Different intracellular trafficking of FGF1 endocytosed by the four homologous FGF receptors. *J Cell Sci*. 118, 3869-3881.
- 15 S. Taverna, S. Rigogliuso, M. Salamone and M. L. Vittorelli. (2008) Intracellular trafficking of endogenous fibroblast growth factor-2. *FEBS J*. 275, 1579-1592.
- 16 C. Bossard, H. Laurell, L. Van den Berghe, S. Meunier, C. Zanibellato and H. Prats. (2003) Translokin is an intracellular mediator of FGF-2 trafficking. *Nat Cell Biol*. 5, 433-439.
- 17 C. Homer-Bouthiette, T. Doetschman, L. Xiao and M. M. Hurley. (2014) Knockout of nuclear high molecular weight FGF2 isoforms in mice modulates bone and phosphate homeostasis. *The Journal of biological chemistry*. 289, 36303-36314.

18 P. Kiefer and C. Dickson. (1995) Nucleolar association of fibroblast growth factor 3 via specific sequence motifs has inhibitory effects on cell growth. *Mol Cell Biol.* 15, 4364-4374.

19 I. Dimauro, T. Pearson, D. Caporossi and M. J. Jackson. (2012) A simple protocol for the subcellular fractionation of skeletal muscle cells and tissue. *BMC Res Notes.* 5, 513.

20 M. K. Hajihosseini and J. K. Heath. (2002) Expression patterns of fibroblast growth factors-18 and -20 in mouse embryos is suggestive of novel roles in calvarial and limb development. *Mech Dev.* 113, 79-83.

21 M. K. Hajihosseini, S. De Langhe, E. Lana-Elola, H. Morrison, N. Sparshott, R. Kelly, J. Sharpe, D. Rice and S. Bellusci. (2008) Localization and fate of Fgf10-expressing cells in the adult mouse brain implicate Fgf10 in control of neurogenesis. *Mol Cell Neurosci.* 37, 857-868.

22 M. Christie, C. W. Chang, G. Rona, K. M. Smith, A. G. Stewart, A. A. Takeda, M. R. Fontes, M. Stewart, B. G. Vertessy, J. K. Forwood and B. Kobe. (2015) Structural Biology and Regulation of Protein Import into the Nucleus. *J Mol Biol.*

23 A. N. Nguyen Ba, A. Pogoutse, N. Provart and A. M. Moses. (2009) NLStradamus: a simple Hidden Markov Model for nuclear localization signal prediction. *BMC Bioinformatics.* 10, 202.

- 24 M. Brameier, A. Krings and R. M. MacCallum. (2007) NucPred--predicting nuclear localization of proteins. *Bioinformatics*. 23, 1159-1160.
- 25 J. Kosman, N. Carmean, E. M. Leaf, K. Dyamenahalli and J. A. Bassuk. (2007) Translocation of fibroblast growth factor-10 and its receptor into nuclei of human urothelial cells. *J Cell Biochem*. 102, 769-785.
- 26 Z. Sheng, J. A. Lewis and W. J. Chirico. (2004) Nuclear and nucleolar localization of 18-kDa fibroblast growth factor-2 is controlled by C-terminal signals. *J Biol Chem*. 279, 40153-40160.
- 27 J. Wesche, J. Malecki, A. Wiedlocha, M. Ehsani, E. Marcinkowska, T. Nilsen and S. Olsnes. (2005) Two nuclear localization signals required for transport from the cytosol to the nucleus of externally added FGF-1 translocated into cells. *Biochemistry*. 44, 6071-6080.
- 28 M. Yamasaki, A. Miyake, S. Tagashira and N. Itoh. (1996) Structure and expression of the rat mRNA encoding a novel member of the fibroblast growth factor family. *J Biol Chem*. 271, 15918-15921.
- 29 H. D. Beer, C. Florence, J. Dammeier, L. McGuire, S. Werner and D. R. Duan. (1997) Mouse fibroblast growth factor 10: cDNA cloning, protein characterization, and regulation of mRNA expression. *Oncogene*. 15, 2211-2218.

- 30 F. Terao, I. Takahashi, H. Mitani, N. Haruyama, Y. Sasano, O. Suzuki and T. Takano-Yamamoto. (2011) Fibroblast growth factor 10 regulates Meckel's cartilage formation during early mandibular morphogenesis in rats. *Dev Biol.* 350, 337-347.
- 31 F. G. Sala, P. M. Del Moral, C. Tiozzo, D. A. Alam, D. Warburton, T. Grikscheit, J. M. Veltmaat and S. Bellusci. (2011) FGF10 controls the patterning of the tracheal cartilage rings via Shh. *Development.* 138, 273-282.
- 32 H. P. Makarenkova, M. P. Hoffman, A. Beenken, A. V. Eliseenkova, R. Meech, C. Tsau, V. N. Patel, R. A. Lang and M. Mohammadi. (2009) Differential interactions of FGFs with heparan sulfate control gradient formation and branching morphogenesis. *Sci Signal.* 2, ra55.
- 33 T. Pederson. (2011) The nucleolus. *Cold Spring Harb Perspect Biol.* 3.
- 34 Z. Sheng, Y. Liang, C. Y. Lin, L. Comai and W. J. Chirico. (2005) Direct regulation of rRNA transcription by fibroblast growth factor 2. *Mol Cell Biol.* 25, 9419-9426.
- 35 K. Reimers, M. Antoine, M. Zapatka, V. Blecken, C. Dickson and P. Kiefer. (2001) NoBP, a nuclear fibroblast growth factor 3 binding protein, is cell cycle regulated and promotes cell growth. *Mol Cell Biol.* 21, 4996-5007.
- 36 M. K. Hajhosseini, R. Duarte, J. Pegrum, A. Donjacour, E. Lana-Elola, D. P. Rice, J. Sharpe and C. Dickson. (2009) Evidence that Fgf10 contributes to the

skeletal and visceral defects of an Apert syndrome mouse model. *Dev Dyn.* 238, 376-385.

37 L. D. Urness, X. Wang, S. Shibata, T. Ohyama and S. L. Mansour. (2015) Fgf10 is required for specification of non-sensory regions of the cochlear epithelium. *Dev Biol.* 400, 59-71.

38 N. Haan, T. Goodman, A. Najdi-Samiei, C. M. Stratford, R. Rice, E. El Agha, S. Bellusci and M. K. Hajihosseini. (2013) Fgf10-expressing tanycytes add new neurons to the appetite/energy-balance regulating centers of the postnatal and adult hypothalamus. *J Neurosci.* 33, 6170-6180.

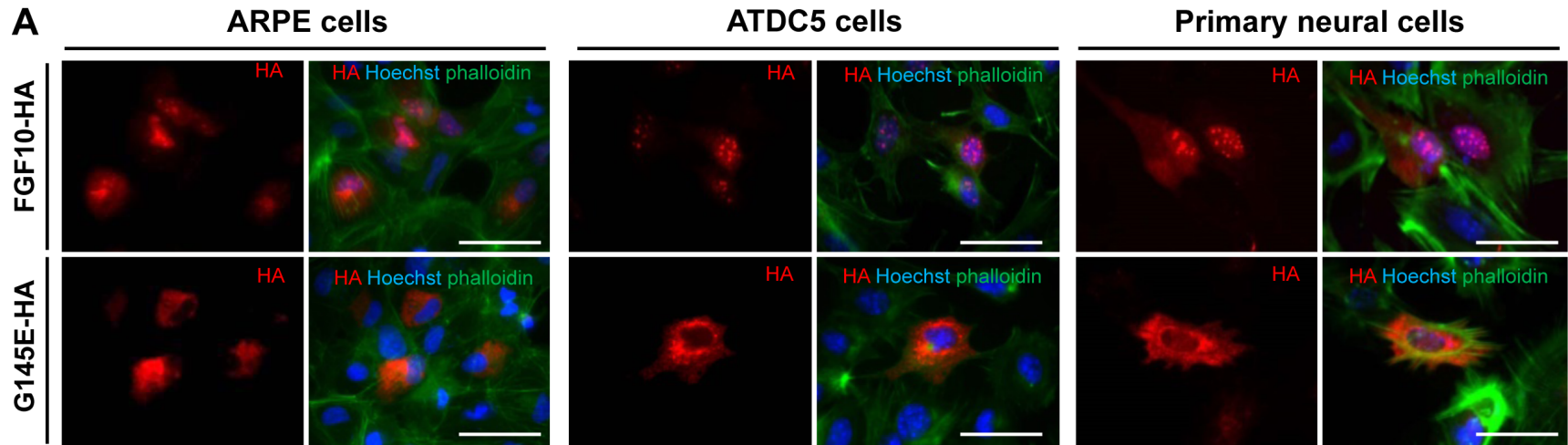
39 F. Seymen, M. Koruyucu, I. R. Toptanci, S. Balsak, S. Dedeoglu, T. Celepkolu, T. J. Shin, H. K. Hyun, Y. J. Kim and J. W. Kim. (2016) Novel FGF10 mutation in autosomal dominant aplasia of lacrimal and salivary glands. *Clin Oral Investig.* In press.

40 E. D. Lew, J. H. Bae, E. Rohmann, B. Wollnik and J. Schlessinger. (2007) Structural basis for reduced FGFR2 activity in LADD syndrome: Implications for FGFR autoinhibition and activation. *Proc Natl Acad Sci U S A.* 104, 19802-19807.

41 K. Scheckenbach, V. Balz, M. Wagenmann and T. K. Hoffmann. (2008) An intronic alteration of the fibroblast growth factor 10 gene causing ALSG-(aplasia of lacrimal and salivary glands) syndrome. *BMC Med Genet.* 9, 114.



# Figure 2



■ Nuclear (N)    ■ Cytoplasmic (C)    □ Equal N/C

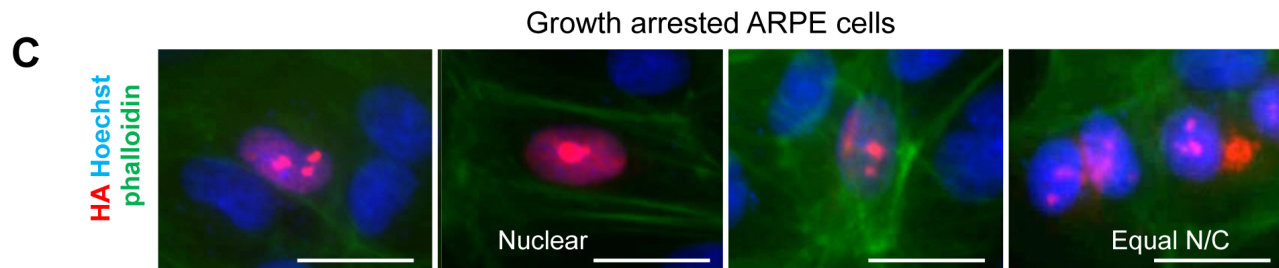
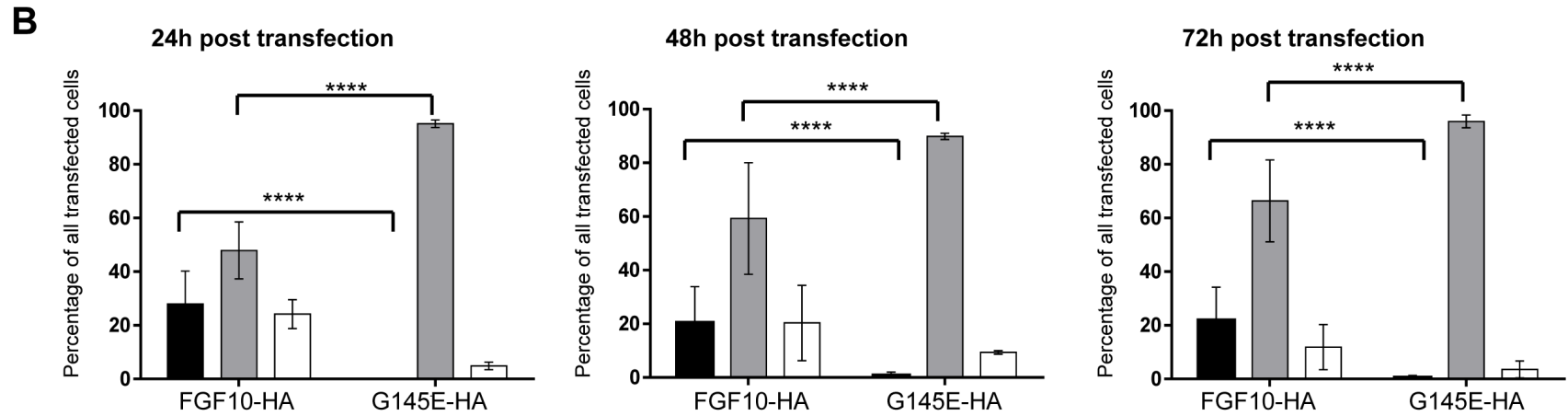
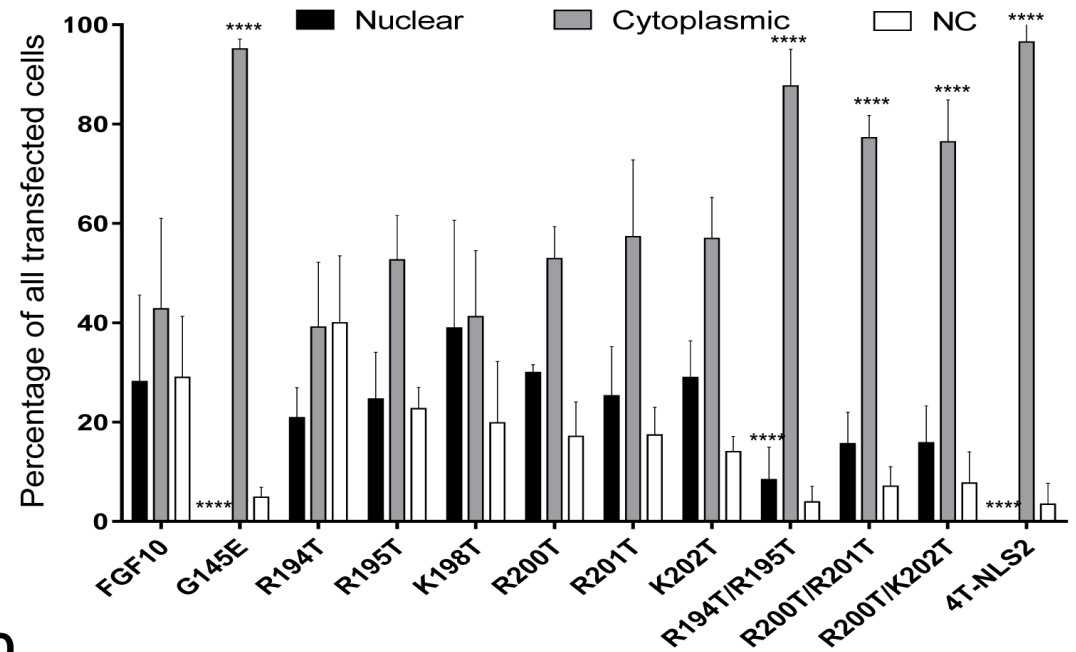


**Figure 3**

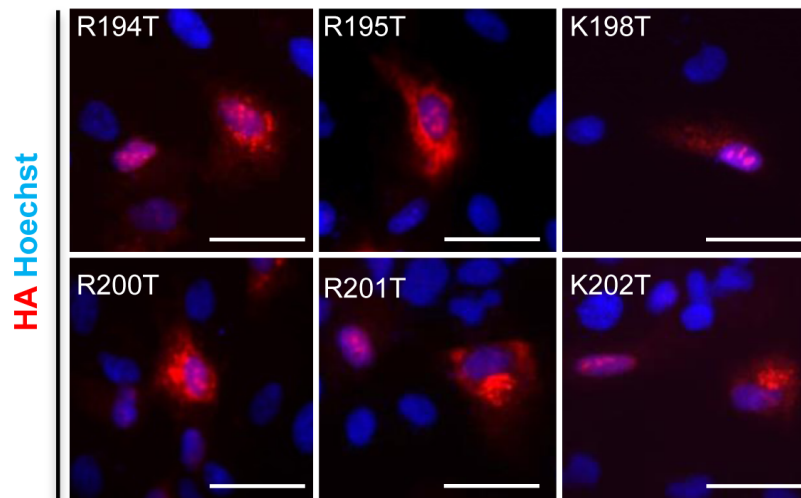
**A**

Site directed mutagenesis	Sequence
Wild type NLS	194 RRGQKTRRK 202
R194T	194 T..... 202
R195T	194 ...T..... 202
K198T	194 .....T..... 202
R200T	194 .....T.... 202
R201T	194 .....T.. 202
K202T	194 .....T 202
R194T/ R195T	194 TT..... 202
R200T/ R201T	194 .....TT.. 202
R200T/K202T	194 .....T..T 202
R194T/ R195T/ R200T/ K202T(4T-NLS2)	194 TT.....T..T 202

**B**



**C**



**D**

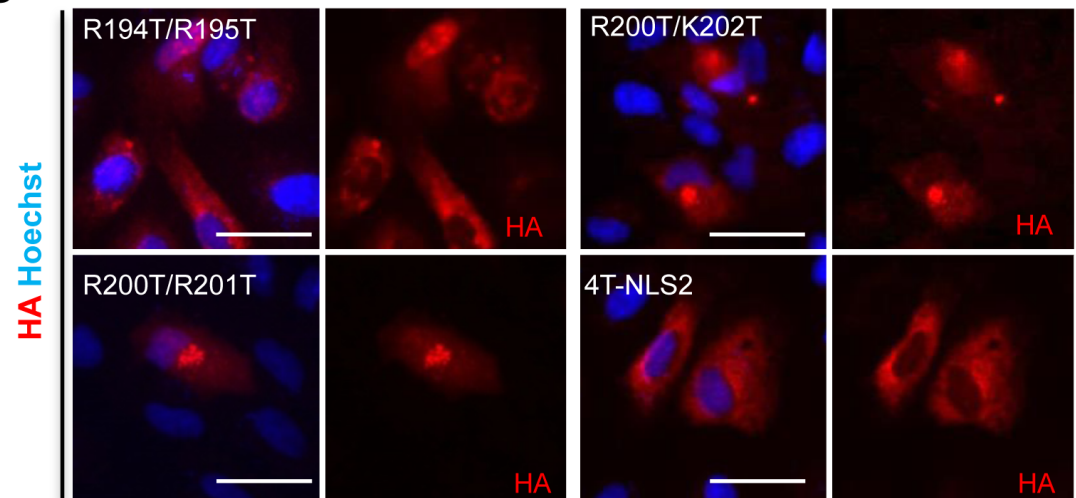




**Figure 5**

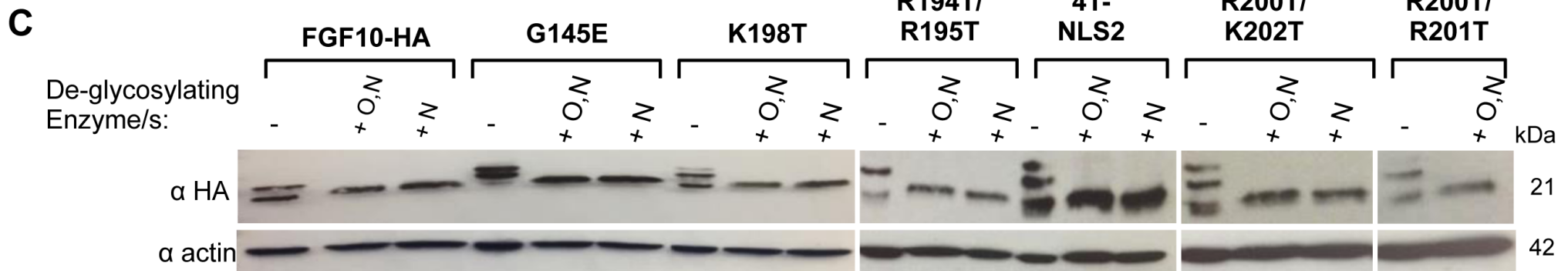
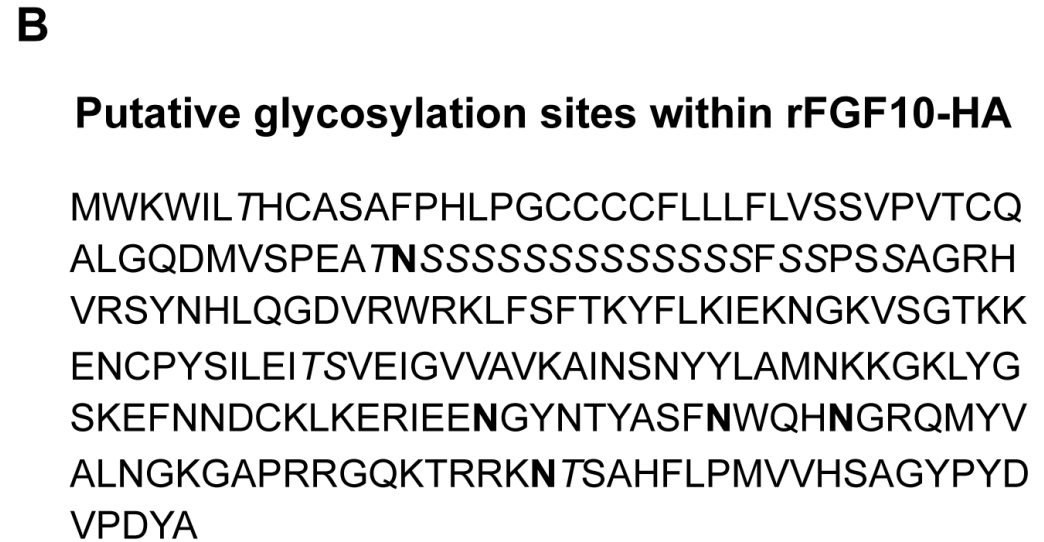
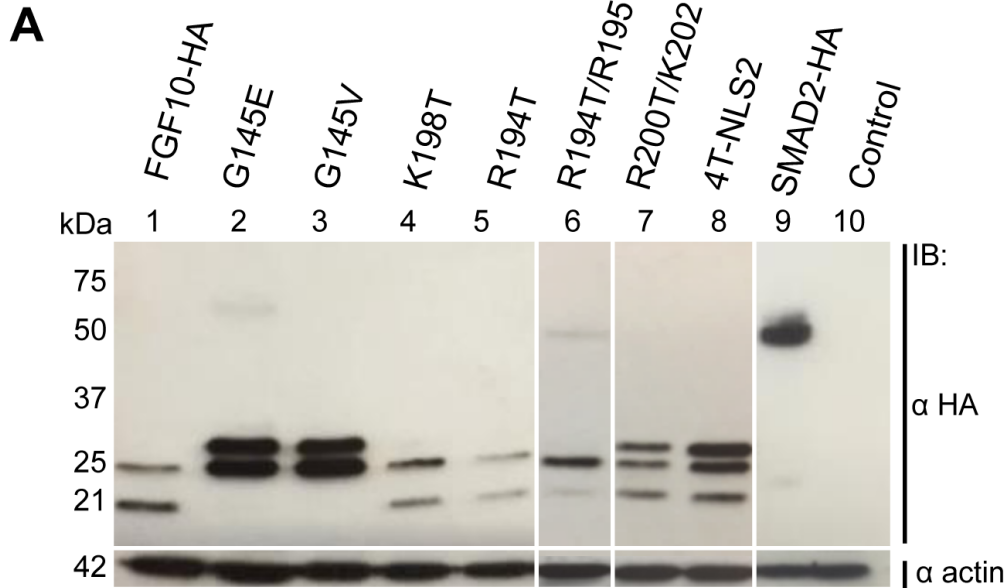
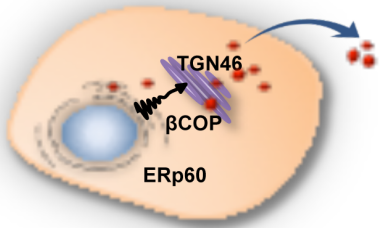
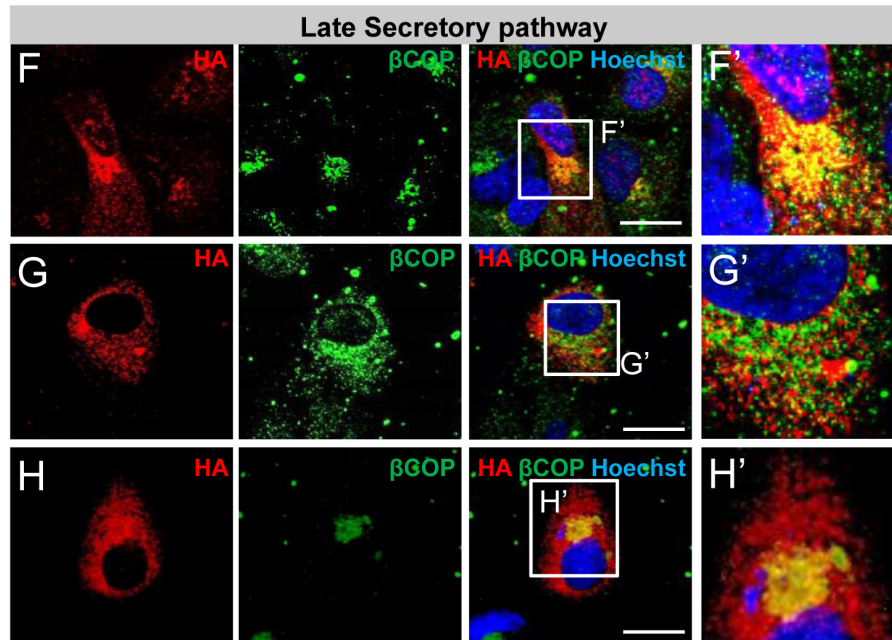
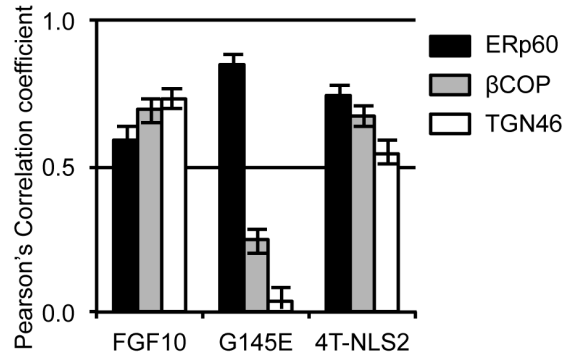


**Figure 6**

**A**



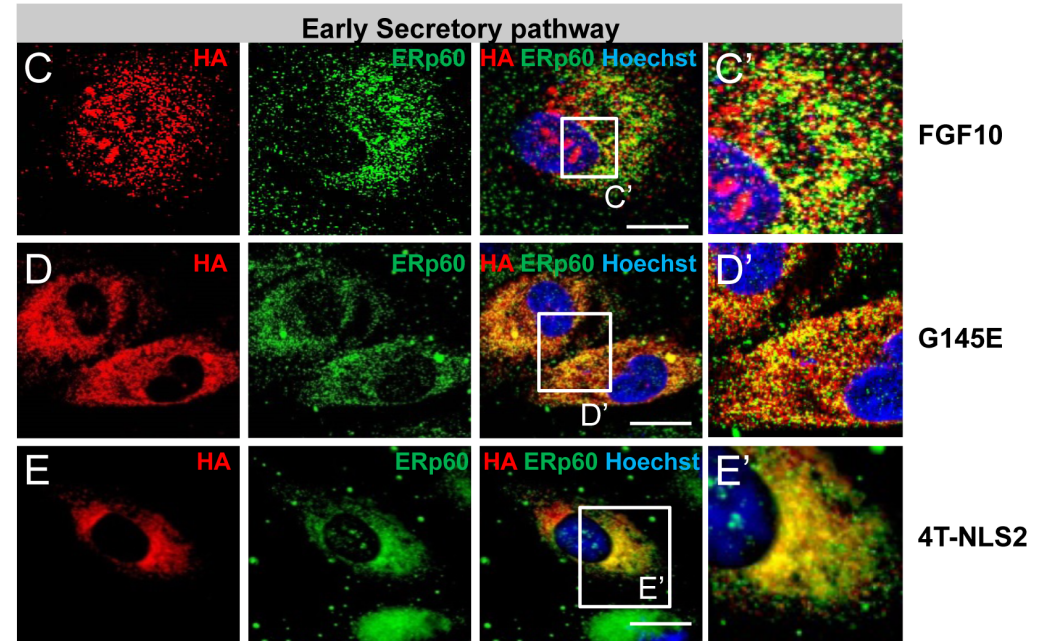
**B**



FGF10

G145E

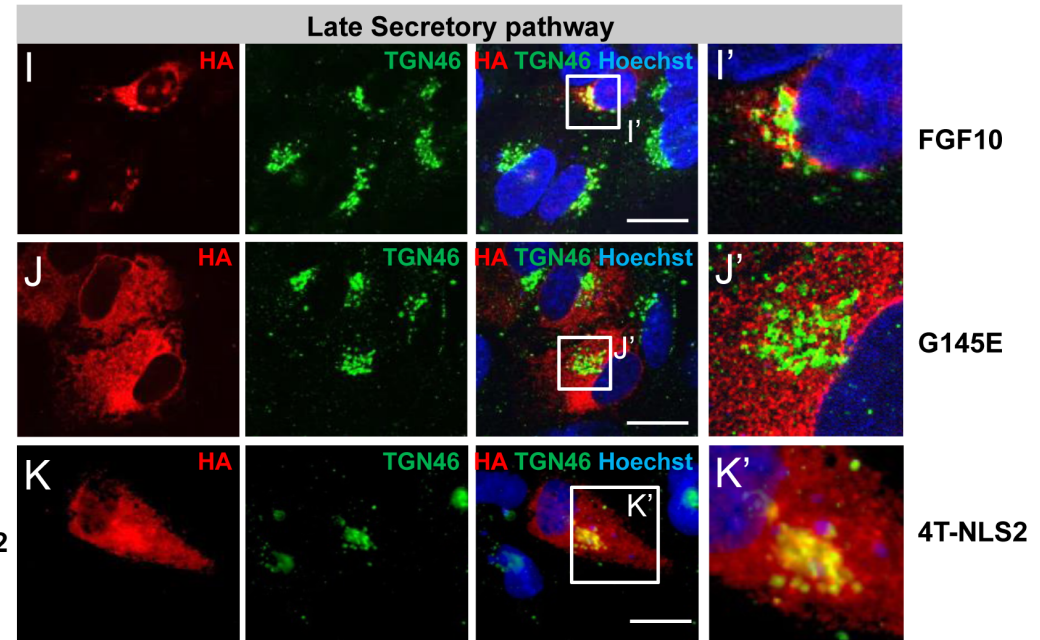
4T-NLS2



FGF10

G145E

4T-NLS2



FGF10

G145E

4T-NLS2

Figure 7

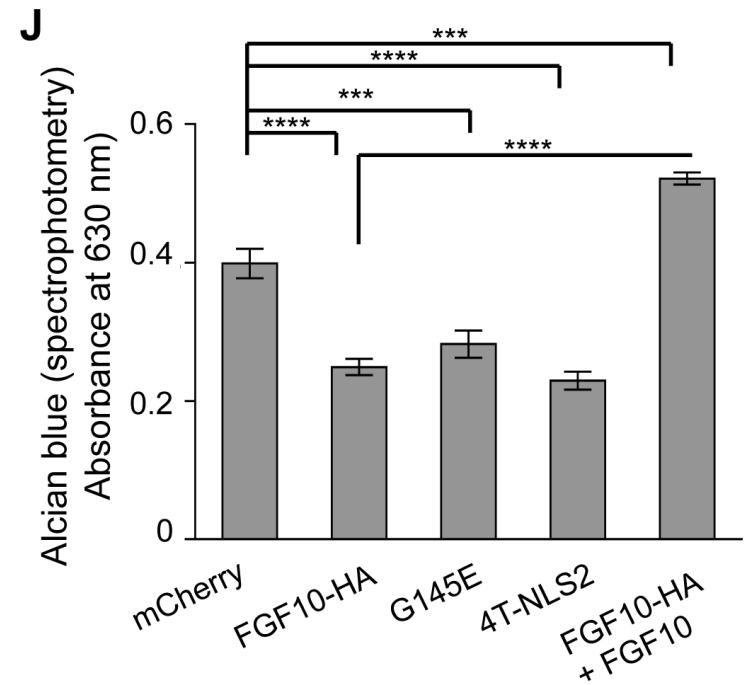
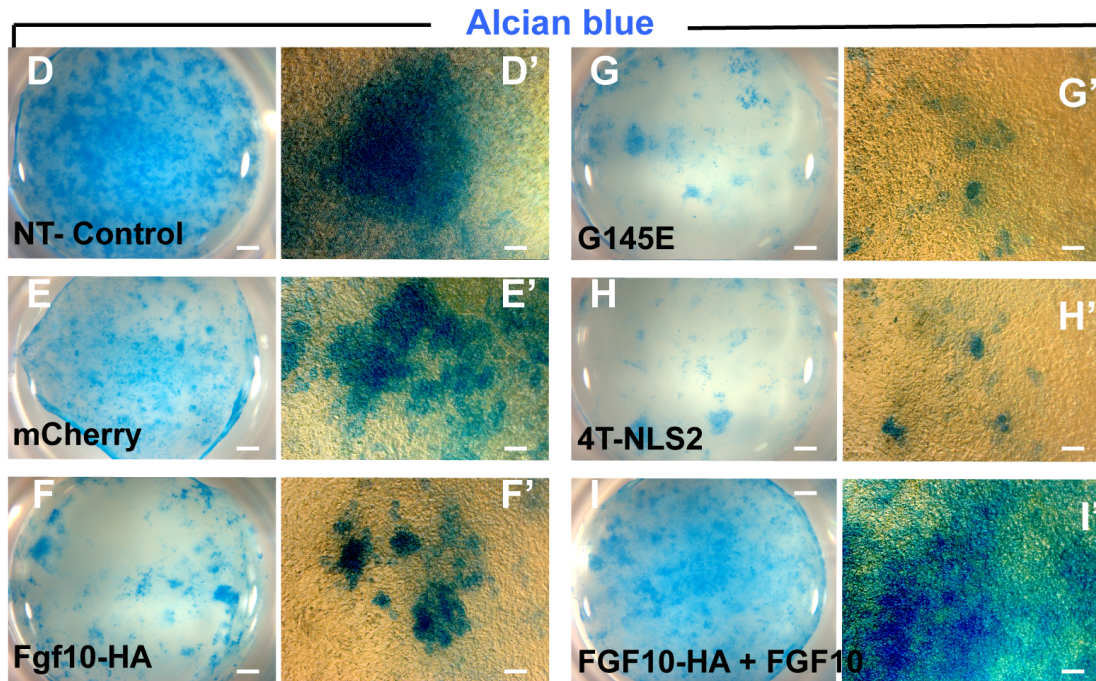
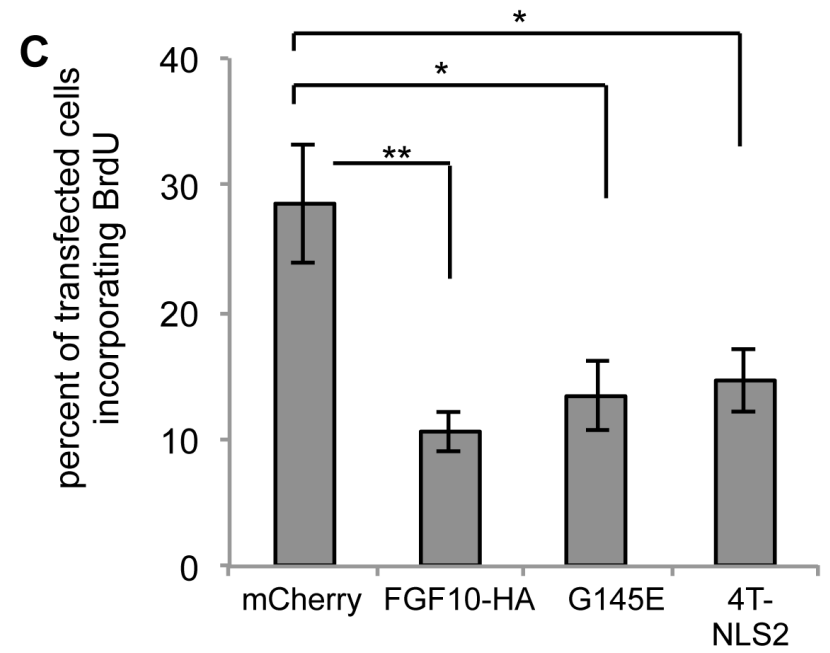
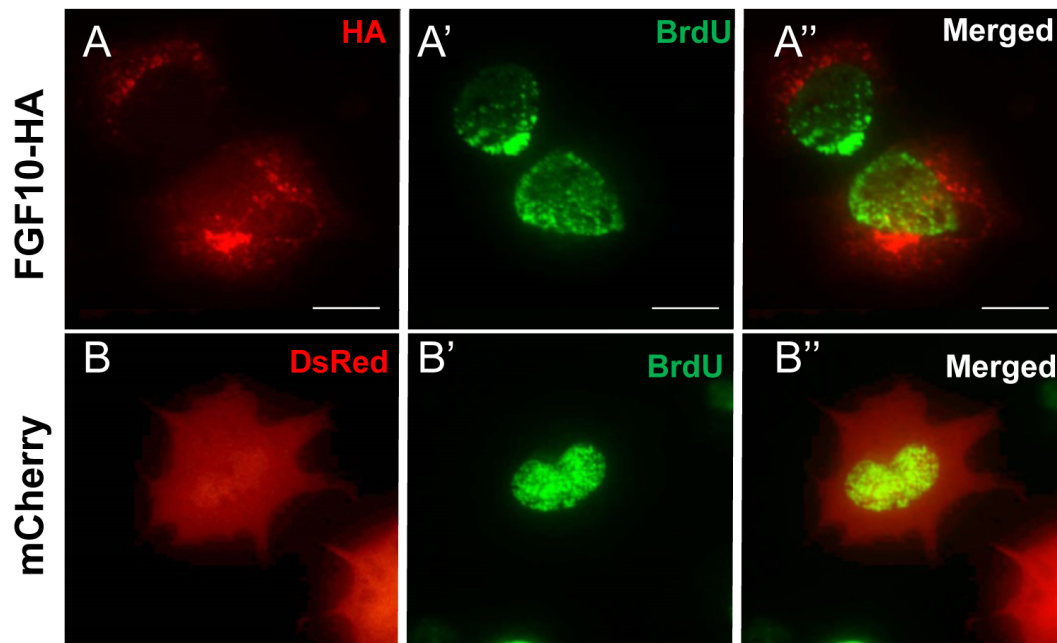


**Table 1. Spectrum of LADD/ALSG syndrome causative mutations**

<b>FGF10 mutations</b>				
<b>Mutation/ Deletion</b>	<b>Amino acid change</b>	<b>Syndrome</b>	<b>Molecular consequence</b>	<b>Reference/s</b>
237G →A (exon 1)	W79X	ALSG	Predicted truncated protein	Seymen et al. 2016
240A →C (exon 1)	R80S	ALSG	Disruption of FGF10/ FGFR2-IIIb binding site	Entesarian et al. 2007 Chapman et al. 2009
317G →T (exon 1)	C106F*	LADD	Product unstable at physiological temperature	Rohmann et al. 2006; Shams et al. 2007
Deletion (of exons 2 and 3)	Not applicable	ALSG	No protein product	Entesarian et al. 2005
409A →T (exon 2)	K137X*	ALSG & LADD	Predicted truncated protein	Milunsky et al. 2006
413G →A (exon 2)	G138E*	ALSG/LADD	Unknown	Entesarian et al. 2007
430G →A (intron 2)	n/a	ALSG	Truncated protein	Scheckenbach et al. 2008
467T →G (exon 2)	I156R	LADD	Disruption of FGF10/ FGFR2-IIIb binding site	Milunsky et al. 2006; Shams et al. 2007
506G →A (exon 3)	W169X*	ALSG	Predicted truncated protein	Milunsky et al. 2006
577C →T (exon 3)	R193X	ALSG	Truncated protein; partial abrogation of FGF10/ FGFR2-IIIb binding	Entesarian et al. 2005
620A →C (exon 3)	H207P	No discernable phenotype	Rare polymorphism	Entesarian et al. 2007
<b>FGFR2 mutations</b>				
<b>Mutation/ Deletion</b>	<b>Amino acid change</b>	<b>Syndrome</b>	<b>Molecular consequence</b>	<b>Reference/s</b>
1882G →A	A628T	LADD	Although within ligand-binding domain, affects tyrosine kinase catalytic activity	Rohmann et al. 2006; Shams et al 2007; Lew et al. 2007
1942G →A (exon 16)	A648T	LADD	Affects ligand binding	Rohmann et al. 2006
Δ1947-AGA-1949 base depletion (exon 16)	R649S & ΔD650	LADD	Affects ligand binding	Rohmann et al. 2006